would give the 12 vertices of an icosahedron and locally icosahedral symmetry, which is, of course, in conflict with periodicity, but as we have seen not with quasi-periodicity.

I thank J. C. Toledano, R. Struikmans and the referee for pointing out relevant references.

References

ALEXANDER, S. & MCTAGUE, J. (1978). *Phys. Rev. Lett.* **41**, 702-705.

BAK, P. (1985*a*). *Phys. Rev. Lett.* **54**, 1517-1519.

BAK, P. (1985*b*). *Phys. Rev. B*, **32**, 5764-5772.

BROWN, H. (1969). *Math. Comput.* **23**, 499-514.

BROWN, H., BÜLOW, R., NEUBÜSER, J., WONDRATSCHEK, H. & ZASSENHAUS, H. (1978). *Crystallographic Groups of Four-Dimensional Space*, p. 285. New York: Wiley.

BRUIJN, N. G. DE (1981). *Proc. K. Ned. Akad. Wet.* **A84**, 39-66.

COXETER, H. S. M. (1961). *Introduction to Geometry*, p. 409. New York: Wiley.

COXETER, H. S. M. (1980). *Unvergängliche Geometrie*, p. 489. Basel: Birkhäuser. (In German.)

DUNEAU, M. & KATZ, A. (1985). *Phys. Rev. Lett.* **54**, 2688-2691.

ELSER, V. (1985). *Phys. Rev. B*, **32**, 4892-4898.

FAST, G. & JANSSEN, T. (1971). *J. Comput. Phys.* **7**, 1-11.

GARDNER, M. (1977). *Sci. Am.* **236**, 110-121.

HALES, S. (1727). *Vegetable Staticks*. London.

JANNER, A. & JANSSEN, T. (1977). *Phys. Rev. B*, **15**, 643-658.

JANNER, A. & JANSSEN, T. (1979). *Physica (Utrecht)*, **99A**, 47-76.

JANSSEN, T. & TJON, J. A. (1983). *J. Phys. C*, **16**, 4789-4810.

JARIC, M. V. (1985). *Phys. Rev. Lett.* **55**, 607-610.

KRAMER, P. (1982). *Acta Cryst.* **A38**, 257-264.

KRAMER, P. (1985). *Z. Naturforsch. Teil A*, **40**, 775-788.

KRAMER, P. & NERI, R. (1984). *Acta Cryst.* **A40**, 580-587.

LEVINE, D. & STEINHARDT, P. J. (1984). *Phys. Rev. Lett.* **53**, 2477-2480.

MACKAY, A. L. (1982). *Physica (Utrecht)*, **114A**, 609-613.

MARVIN, J. W. (1939). *Am. J. Bot.* **26**, 208-288.

MATZKE, E. B. (1950). *Bull. Torrey Bot. Club*, **77**, 222-227.

MERMIN, N. D. & TROIAN, S. M. (1985). *Phys. Rev. Lett.* **54**, 1524-1527.

PENROSE, R. (1974). *Bull. Inst. Math. Appl.* **10**, 216.

ROGERS, C. A. (1958). *Proc. London Math. Soc.* (3) **8**, 609-620.

SHECHTMAN, D., BLECH, I., GRATIAS, D. & CAHN, J. W. (1984). *Phys. Rev. Lett.* **53**, 1951-1954.

STEINHARDT, P. J., NELSON, D. R. & RONCHETTI, M. (1983). *Phys. Rev. B*, **28**, 784-805.

WOLFF, P. M. DE (1977). *Acta Cryst.* **A33**, 493-497.

WOLFF, P. M. DE, JANSSEN, T. & JANNER, A. (1981). *Acta Cryst.* **A37**, 625-636.

ZASSENHAUS, H. (1948). *Commun. Math. Helv.* **21**, 117-141.

Acta Cryst. (1986). A**42**, 271-281

The Electron Distribution in Silicon. A Comparison between Experiment and Theory

BY MARK A. SPACKMAN*

Department of Physics, University of Western Australia, Nedlands, Western Australia 6009

(*Received* 20 *June* 1985; *accepted* 3 *Feburary* 1986)

Abstract

Deformation and valence-electron densities in silicon are derived *via* Fourier summation and multipole refinement of highly accurate measurements of X-ray structure factors. These results provide a new perspective for the comparison between theory and experiment. The model electron density derived from experiment is in quantitative agreement with recent solid-state calculations, but not with earlier experimental results reported by Yang & Coppens [*Solid State Commun.* (1974), **15**, 1555-1559].

Introduction

Experimental electron distributions for crystalline silicon have been the subject of numerous investigations [*e.g.* see Scheringer (1980), Fehlmann (1979), Price, Maslen & Mair (1978; referred to below as PMM), Yang & Coppens (1974; referred to as YC), Aldred & Hart (1973; referred to as AH) and references therein]. In this work we take advantage of recent highly accurate experimental reports on silicon, which, in combination with the earlier measurements of AH, provide data sets of extraordinarily high quality.

The important 222 reflection in silicon was remeasured by Alkire, Yelon & Schneider (1982), with an accuracy better, by a factor of between two and ten, than previous measurements. Alkire *et al.* report F_{222} at room temperature with an accuracy of 0·5%, a measurement of accuracy similar to the AH data (~0·1%).

Teworte & Bonse (1984) measured silicon structure factors for 16 reflections at room temperature with both Ag $K\alpha_1$ and Mo $K\alpha_1$ radiations which were also used by AH. Teworte & Bonse's work verified AH's measurements, and confirmed the claimed accuracy

* Present address: Department of Crystallography, University of Pittsburgh, Pittsburgh, PA 15260, USA.

0108-7673/86/040271-11$01.50

of 0·1% or better. They also measured two reflections (551 and 300) not reported by AH.

Other recent experimental results include the magnitude and phase of the 442 and 622 reflections by Tischler & Batterman (1984), and a measurement to an accuracy of better than 1 in 10^9 of the refractive index of silicon by Deutsch & Hart (1984). This latter work provides values of the real part of the dispersion corrections for Ag $K\bar{\alpha}$ and Mo $K\bar{\alpha}$ with accuracies of better than 5%.

Combination of these measurements with those of AH provides extensive data at two wavelengths, which are more accurate than any previously analysed. Here we take advantage of these superb data, providing a new perspective for a comparison between experiment and theory, as recently suggested by Alkire *et al.* (1982).

We analyse combined data sets, at two wavelengths, pursuing both Fourier methods, as used by YC, and a rigid pseudoatom model (Stewart, 1973, 1976) to explore the effects of series termination and thermal motion. Where possible, standard deviations (e.s.d.'s) in the results are determined from the errors in the experimental observations, and the curvature of the least-squares error surface at the minimum.

The data sets

A weighted mean of the measurements of AH and Teworte & Bonse (1984) was calculated for the reflections measured twice at each wavelength (Mo $K\alpha_1$ and Ag $K\alpha_1$). The measurements of AH were corrected for the more precise lattice constant, $a_0 = 5{\cdot}43102018\ (39)$ Å (Becker, Seyfried & Siegert, 1982) in the manner of Teworte & Bonse (1984). The variance in the mean was used to estimate standard deviations for the data. Measurements reported by only one group were added to the mean data. In this manner data sets of 17 reflections were obtained for each wavelength. To these were added the 222 measurement of Alkire *et al.* (1982), and the observations of 442 and 622 by Tischler & Batterman (1984). All observations were either measured at, or converted to, room temperature (between 293 and 298 K). Although the 222, 442 and 622 reflections were measured at wavelengths different to either Ag $K\alpha_1$ or Mo $K\alpha_1$, none of these reflections have significant contributions from anomalous dispersion, and no problem arises from the inclusion of the measurements of these reflections in both data sets.

The raw data thus consist of 20 measurements for each radiation. The data are complete out to $\sin\theta/\lambda = 0{\cdot}52$ Å^{-1} (440), and incomplete up to a maximum of $1{\cdot}04$ Å^{-1}. A complete data set with $\sin\theta/\lambda < 1{\cdot}05$ Å^{-1} would include 51 reflections. No attempt was made to incorporate structure factors measured by Hattori, Kuriyama, Katagawa & Kato (1965; referred to as HKKK) but not by AH. These measurements are not as accurate as those discussed above [$\sigma(F) \sim 1{\cdot}4\%$] and, as indicated by Scheringer (1980), do not have the accuracy necessary to determine $\Delta\rho$ to better than $0{\cdot}02$ e Å^{-3}. Their inclusion would compromise the efforts made in this work to obtain a representation of $\rho(\mathbf{r})$ commensurate with the accuracy of the other data.

In both Fourier mapping and the least-squares refinements the structure factors were corrected for anomalous dispersion using the real dispersion corrections f', measured for Ag $K\bar{\alpha}$ and Mo $K\bar{\alpha}$ radiations by Deutsch & Hart (1984). The differences between values at these mean wavelengths and those appropriate to the $K\alpha_1$ radiation are very small, being 15% of the e.s.d.'s in f' reported by Deutsch & Hart. These f' values are substantially larger than the conventional values obtained theoretically by Cromer & Liberman (1970). However, they are in excellent agreement with other measurements of f' in Si by Creagh (1984) and by Cusatis & Hart (1975). Since nuclear Thomson scattering behaves in a manner identical to f' corrections, we added $0{\cdot}0038$ to the experimental f' values, a nuclear scattering correction appropriate to Si. The combined correction values used were $0{\cdot}0575$ (Ag) and $0{\cdot}0885$ (Mo). No angle dependence was assumed for f', apart from the Debye–Waller factor.

Within the convolution approximation the atomic scattering factor is multiplied by a temperature factor which is the Fourier transform of the nuclear probability distribution function. The temperature factor is due both to harmonic and anharmonic atomic vibrations. In view of the $\bar{4}3m$ site symmetry of the Si atoms the harmonic term, $\exp[-B(\sin\theta/\lambda)^2]$, is isotropic, and the dominant anharmonic effect is the cubic term (Dawson, Hurley & Maslen, 1967; Willis & Pryor, 1975). The data were corrected for anharmonic effects in the manner described in detail by PMM and Fehlmann (1979). The cubic anharmonic force constant employed was $\beta = 3{\cdot}38$ eV Å^{-3} ($5{\cdot}42 \times 10^{11}$ J m^{-3}), obtained from the room-temperature neutron 222 reflection (Roberto, Batterman & Keating, 1974; Keating, Nunes, Batterman & Hastings, 1971). This value of β was also used by Fehlmann (1979) and PMM. It is much larger than the near-constant value of $\sim 1{\cdot}67$ eV Å^{-3} reported by Roberto *et al.* (1974) at higher temperatures, the values of $1{\cdot}61$ and $1{\cdot}38$ eV Å^{-3} obtained by Hastings & Batterman (1975) from the temperature dependence of the neutron 442 and 622 reflections, and values of $1{\cdot}65$ and $1{\cdot}41$ eV Å^{-3} obtained by Tischler & Batterman (1984) from the temperature dependence of the X-ray 442 and 622 reflections. The consequences of these differences in β are discussed below.

The anharmonic correction applies only to reflections for which $h+k+l = 4n$, and since it is proportional to the product hkl, only to those reflections for which $hkl \neq 0$. Thus only eight reflections require

correction, the largest effect being for 555, where the correction increases $|F|$ by about $3\sigma(|F|)$. The magnitude of the critical 222 structure factor is increased by almost $2\sigma(|F|)$, to a value of 1·470(9). $\sigma(|F|)$ values were adjusted to incorporate the 10% experimental error in β. Anharmonicity-corrected values of the 442 and 622 structure factors were taken from Table II of Tischler & Batterman (1984) [$F^{\rm bond}_{\rm Si(442)}$ and $F^{\rm bond}_{\rm Si(622)}$ in that table].

Analyses of the data

A rigid pseudoatom model was employed to obtain a minimally biased estimate of the isotropic thermal parameter, B, and a deconvolution of the electron distribution from its thermal motion. The nomenclature used here follows that outlined by Stewart (1973, 1976). Although Scheringer (1980) has demonstrated that a simple model of atomic cores and Gaussian-distributed charge clouds placed at the centre of bonds gives an expedient description of the accumulation of charge in some covalent bonds, it is clear from Spackman & Maslen (1985) that there is no necessity for electron density to accumulate between any pair of bonded atoms, including covalently bonded atoms. It is therefore desirable to use some form of multipole expansion to fit the electron density in the most unbiased manner possible.

For the cubic site symmetry of the Si atom in the diamond structure, the allowed multipoles up to fourth order are monopole, octopole and hexadecapole (Dawson, 1967). In Stewart's notation, the allowed multipoles are o_4, h_1 and h_9, each with variable populations, $O4$, $H1$ and $H9$, with the constraint $H1 = H9$.

With data as accurate as those considered here, the choice of radial functions is crucial. For the monopole we use the density-localized K and L shells obtained by Stewart (1980) from the Hartree–Fock atomic wavefunction of Clementi (1965). In previous analyses of silicon X-ray data, AH, PMM and Fehlmann (1979) conclude that allowance for spherical deformation of the valence electron density is important for an adequate description of the structure factors. We therefore choose an M-shell electron density with variable κ which allows expansion or contraction of the electron density (Coppens, Guru Row, Leung, Stevens, Becker & Yang, 1979). We use the density-localized M-shell function compatible with the K and L shells above. This choice of density-localized monopole shells facilitates comparison of the results with theory, as the M shell is essentially nodeless, and very similar to the radial wavefunctions obtained from pseudopotential calculations [*e.g.* see Fig. 2 of Yin & Cohen (1982)]. Jacobi fits to these and the corresponding canonical orbital scattering factors for first- and second-row atoms have been reported by van der Wal & Stewart (1984).

As all experimental data are on an absolute scale, no variable monopole populations or scale factors were included in the refinements. Octopole and hexadecapole radial functions are single exponential, $r^n \exp(-\alpha_l r)$, with $n = 4$ for both higher multipoles. Initially the radial exponents, α_3 and α_4, were varied separately, but it was evident that although α_3 was well determined by the data, α_4 refines to a value close to α_3, with a large e.s.d. It was decided to constrain $\alpha_3 = \alpha_4 = \alpha$.

The model structure factors, F^c_H, were constructed from a model with five variables: B, $O4$, $H1 = H9$, κ and α. The optimum values of these were obtained by minimization of the residual

$$\varepsilon = \sum_H w_H (|F^o_H|^2 - |F^c_H|^2)^2,$$

with $w_H = \sigma^{-2}(|F^o_H|^2)$, $|F^o_H|$ being the observed structure-factor magnitudes. The minimization procedure used is as outlined by Spackman & Stewart (1984, 1986). Convergence to a local minimum was tested by inclusion of second derivatives in the final least-squares cycle. The convergence criterion described in those works is satisfied for all refinements, and e.s.d.'s reported below are from inverse least-squares matrices including second derivatives.

Results of the refinements for the Ag and Mo data sets are given in Table 1. The refined parameters from the two data sets agree with one another to within their respective e.s.d.'s in all cases, an impressive verification of their quality. The value of B is sensitive to the form of the core scattering factors used in its derivation. The mean B value obtained here, 0·4632 (11) Å^2, although slightly lower than typical values obtained by PMM, is in excellent agreement with the value of 0·461 (3) Å^2 obtained by AH.

The mean value of κ, the valence monopole expansion/contraction parameter, is 0·951 (7), reflecting an approximate 5% expansion of the valence electron density. Valence-shell expansion of a similar magnitude (6·8%) was derived in a different manner by AH. In the analysis of a slightly different data set, Fehlmann (1979) used the same M-shell model as AH, obtaining an expansion of 5·3%. Hansen & Coppens (1978) also performed a κ refinement on a combined silicon data set, obtaining $\kappa = 0{\cdot}956\,(9)$ for a canonical M-shell function.

The exponent of the octopole and hexadecapole radial functions, α, has a mean value of 2·36 (4) a.u.$^{-1}$, and is comparable with values obtained by PMM (2·2 to 2·7 a.u.$^{-1}$). It is similar to values of 2·25 (11) and 2·35 (11) a.u.$^{-1}$ obtained by Spackman, Hill & Gibbs (1986) for the silicon radial functions in a pseudoatom refinement of X-ray data on stishovite, SiO_2.

The values of ε at the minima, given in Table 1, suggest that the model fits the Mo data better than

Table 1. *Results of pseudoatom refinements of composite* Ag *and* Mo *data sets for silicon*

	Ag	Mo
B (Å^2)	0·4638 (12)	0·4625 (10)
κ	0·9467 (72)	0·9543 (62)
α (a.u.$^{-1}$)	2·345 (44)	2·371 (40)
*O*4	−0·446 (46)	−0·432 (40)
*H*9	−0·098 (17)	−0·105 (15)
ε	74·31	52·40
g.o.f.	2·23	1·87
$R(F)$ (%)	0·13	0·10
$wR(F)$ (%)	0·24	0·25
$R(F^2)$(%)	0·21	0·17
$wR(F^2)$ (%)	0·27	0·23

Table 2. *Residuals,* $\Delta|F_H| = |F_H^o| - |F_H^c|$, *after pseudoatom refinement of the* Ag *and* Mo *data sets*

	Ag		Mo	
$h\ k\ l$	$\Delta\|F\|$	Δ/σ	$\Delta\|F\|$	Δ/σ
1 1 1	0·001	0·1	−0·005	−0·2
2 2 0	−0·109	−3·2	−0·075	−1·8
3 1 1	−0·030	−1·2	−0·034	−1·3
2 2 2	−0·001	−0·2	0·002	0·2
4 0 0	−0·048	−1·7	−0·074	−2·5
3 3 1	−0·022	−1·1	−0·086	−4·1
4 2 2	−0·121	−4·0	−0·002	−0·1
3 3 3	−0·049	−2·2	−0·035	−1·9
5 1 1	−0·032	−1·6	0·007	0·3
4 4 0	−0·010	−0·4	−0·039	−1·8
4 4 2	−0·028	−7·9	−0·031	−8·9
6 2 2	−0·021	−10·3	−0·022	−10·9
4 4 4	−0·015	−0·8	0·008	0·3
5 5 1	−0·012	−0·5	−0·024	−1·3
6 4 2	0·006	0·1	0·047	0·8
8 0 0	−0·068	−2·1	−0·003	−0·1
6 6 0	0·022	1·4	0·039	2·6
5 5 5	0·063	3·3	0·055	2·1
8 4 4	0·022	1·0	0·030	1·1
8 8 0	0·083	3·8	0·015	0·6

the Ag data. This is reflected in the substantially larger goodness-of-fit (g.o.f.) and R factors for the Ag data. Table 2 gives the residuals, $\Delta|F|$, and the ratio $\Delta|F|/\sigma(|F|)$, for both multipole refinements. For all reflections except the 442 and 622 (which we discuss below), the square of the ratio $\Delta|F|/\sigma(|F|)$ is a good approximation to the contribution of that reflection to ε.

It is evident from Table 2 that four reflections (220, 422, 555 and 880) comprise 70% of ε for the Ag refinement. These same reflections comprise only 16% of ε for the Mo refinement. There is nothing systematic about the size of the discrepancies in the two cases. For example, $\Delta|F|/\sigma(|F|)$ for 422 and 880 is large for one data set, and small for the other. However, there is an overall systematic trend in the residuals; $\Delta|F|$ is close to zero for very low $\sin\theta/\lambda$, becomes increasingly negative, then approaches zero and becomes positive for high $\sin\theta/\lambda$. This behaviour, evident in both refinements, indicates very small features not accounted for by the pseudoatom model.

To explore this in more detail, we map the residual electron density obtained by Fourier summation of $F_H^o - F_H^c$ for the Ag and Mo data sets in Fig. 1. The contour interval of 0·005 e Å^{-3} reflects the size of the e.s.d.'s derived from the experimental errors in $|F_H^o|$ (typically between 0·004 and 0·006 e Å^{-3} for both data sets). Features exceeding two or three contour levels may be regarded as significant. Although there are several such features in both maps, the only substantial features *common to both maps* are those around the nuclei. These are depressions with depths of −0·031 (6) e Å^{-3} in the Ag data map, and −0·019 (5) e Å^{-3} for the Mo data. In both cases the minima occur in directions parallel to the map axes (*i.e.* [100] and [110]), and away from the nuclei, which are located on local maxima. Another feature common to both maps in Fig. 1 is the peak behind the nuclei, reaching 0·013 (5) and 0·010 (4) e Å^{-3} in the Ag and Mo maps respectively.

Several explanations might be proposed for these features. These include incorrect corrections for anomalous dispersion, and erroneous or incomplete anharmonicity corrections. However, if we assume that the measurements of f' by Deutsch & Hart (1984) are appropriate, and the description of anharmonicity within the one-particle-potential approximation of Dawson *et al.* (1967) holds at room temperature, it is plausible that these small systematic residuals are due to polarization of the L shell, which, although small, necessarily exists. The typical residuals summing to give these features are of the order of one to two e.s.d.'s. From Table 2 it appears that there are random errors in both sets of data of as much as $3\sigma(|F|)$. Even data of this quality are not sufficiently

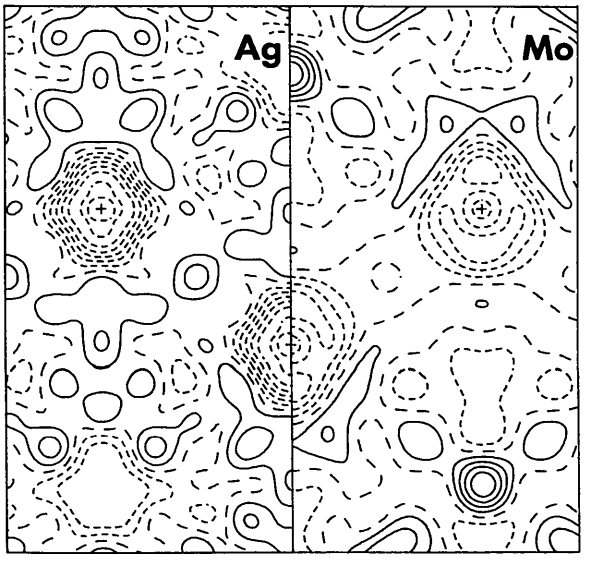

Fig. 1. Residual electron density maps after multipole refinement of the Ag and Mo data. Nuclear positions are marked with a+. The contour interval is 0·005 e Å^{-3}, with zero and negative contours shown as dashed lines. The map is $3\sqrt{2}a_0/4$ horizontally (along [110]) and a_0 vertically.

accurate to determine the origin of very small systematic residuals. In summary, we note that in the vicinity of the nuclei the model does not fit the data as well as it does elsewhere. The *maximum* effect this may have on the electron density is of the order of 0·02 e Å^{-3}, in a region within ~0·4 Å of the nuclei.

Fourier maps

In this section we discuss the deformation electron density, $\Delta\rho(\mathbf{r})$, and the valence electron density, $\rho_{\rm val}(\mathbf{r})$, obtained from Fourier summations. For $\Delta\rho(\mathbf{r})$ the Fourier coefficients are $F_H^o - F_H^{\rm IAM}$, where $F_H^{\rm IAM}$ is obtained from the independent atom model (IAM) using the atomic wavefunction from Clementi (1965). For the calculation of $\rho_{\rm val}(\mathbf{r})$, we sum $F_H^o - F_H^{\rm core}$, where $F_H^{\rm core}$ is calculated from the density-localized K- and L-shell functions of Stewart (1980). B values from Table 1 are employed in both cases. The phases of the Fourier coefficients are those of F_H^c from the pseudoatom model.

Fig. 2 shows maps of $\Delta\rho(\mathbf{r})$ from both data sets. They are quantitatively similar, characterized by elliptical bond peaks reaching 0·213 (6) and 0·204 (6) e Å^{-3} and deficits of electron density behind the nuclei (along [111]) as deep as −0·071 (5) and −0·066 (4) e Å^{-3} for the Ag and Mo data respectively. As discussed above, experimental e.s.d.'s in both maps are typically between 0·004 and 0·006 e Å^{-3}. The maximum deviations between the two maps occur in regions away from the bond midpoint, either at the nuclei, $(\frac{1}{8},\frac{1}{8},\frac{1}{8})$, or at $(\frac{3}{8},\frac{3}{8},\frac{3}{8})$ and symmetry-related positions (the site of the large peaks in Fig. 1 for the Mo data set). They are at most 0·033 e Å^{-3}. These differences are largely due to those reflections which are poorly fitted in one pseudoatom refinement but not in the other, and are hence most likely to be in error experimentally.

The addition of the density-localized M-shell functions to the maps in Fig. 2 gives the maps of the Fourier-summed valence density in Fig. 3. The agreement between the two maps in Fig. 3 should be identical to that between maps in Fig. 2. The Fourier valence density has local minima at the nuclei, rectangular-shaped bond contours, elongated along the bond, with a single peak at the bond midpoint, and a local maximum behind each nucleus. The bond peaks are 0·617 (6) and 0·609 (6) e Å^{-3} and the peaks behind the nuclei 0·396 (4) and 0·390 (4) e Å^{-3} for the Ag and Mo data respectively.

Maps from pseudoatom summations

Assuming an adequate representation of thermal motion, we may assume $B = 0$ and map any subset of the electron density function without thermal motion, within the convolution approximation. In this manner we map in Figs. 4 and 5 $\Delta\rho(\mathbf{r})$ and $\rho_{\rm val}(\mathbf{r})$ corrected for vibrational effects.

The maps of $\Delta\rho$ and $\rho_{\rm val}$ derived from the pseudoatom refinement to the Ag and Mo data sets are virtually identical, as expected from the results in Table 1. The *maximum* difference between the model electron densities derived from the two data sets is only 0·010 e Å^{-3}. When compared with the typical e.s.d.'s in these functions of between 0·003

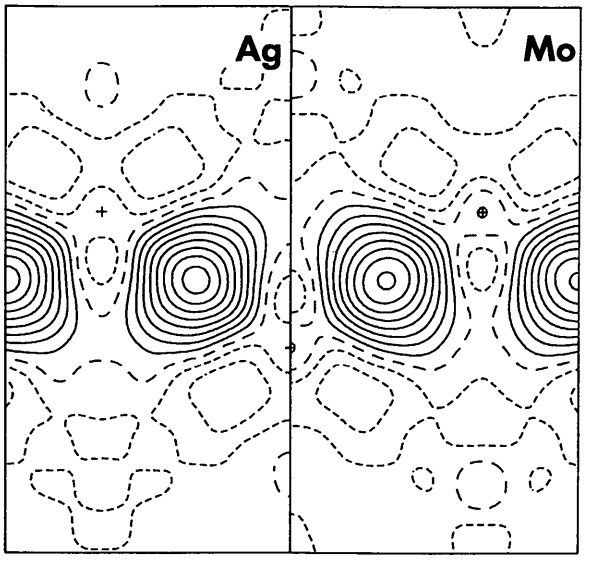

Fig. 2. Deformation electron densities, $\Delta\rho(\mathbf{r})$, obtained by Fourier summation, for both the Ag and Mo data. Nuclear positions are marked with a+. The contour interval is 0·025 e Å^{-3}, with zero and negative contours dashed. Map dimensions as in Fig. 1.

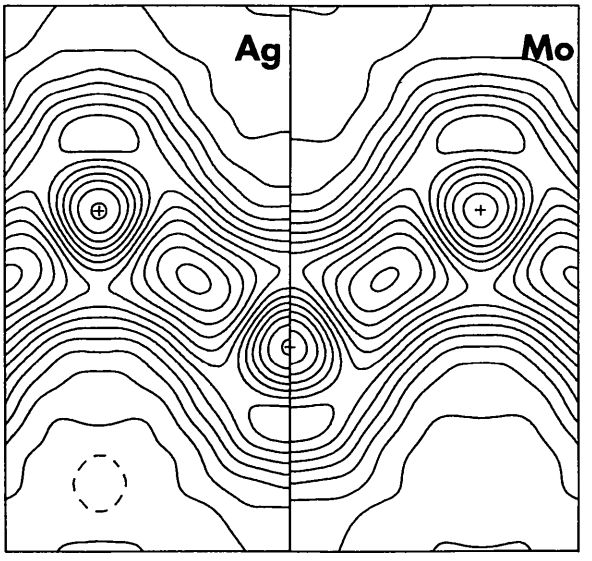

Fig. 3. Valence electron densities, $\rho_{\rm val}(\mathbf{r})$, obtained by Fourier summation, for both the Ag and Mo data. Nuclear positions are marked with a+. The contour interval is 0·05 e Å^{-3}, with the zero contour dashed. Map dimensions as in Fig. 1.

and 0·005 e Å^{-3}, this maximum difference of at most 3σ reinforces our expectation that such e.s.d.'s are reliable estimates of the reproducibility of the model results. We contour $\Delta\rho$ and ρ_{val} with intervals of 0·025 and 0·05 e Å^{-3} respectively, far in excess of the e.s.d.'s. Figs. 4 and 5 display maps of $\Delta\rho$ and ρ_{val} from pseudoatom refinements of both the Ag and Mo data sets, to emphasize the excellent agreement between the two results.

The static model $\Delta\rho(\mathbf{r})$ maps in Fig. 4 reproduce the features in Fig. 2 in all respects. The discernible differences are, as expected, in the vicinity of the nuclei, where the model exceeds the Fourier-summation result, and beyond the nuclei, away from the bonds, where the model yields deeper hollows. Peak heights are 0·205 (4) and 0·206 (3) e Å^{-3}, and hollows −0·093 (4) and −0·086 (4) e Å^{-3} for $\Delta\rho$ obtained from the Ag and Mo data sets respectively. Clearly the effect of thermal motion on the results in Fig. 2 is minimal.

The static model valence-electron density maps in Fig. 5 are qualitatively similar to those in Fig. 3, but differ in some respects. The model maps have tighter contours around the nuclei, due largely to the lack of thermal motion in the model maps. The Fourier maps display erratic behaviour at large distances from the nuclei, and in the case of the Ag data exhibit regions of negative electron density. This is not the case for the static maps in Fig. 5, indicating that these features in Fig. 3 were caused by thermal motion and/or series termination (*i.e.* the limited number of high-angle reflections).

The most important difference between the maps in Fig. 3 and those in Fig. 5 is the presence of twin bond peaks in both maps in Fig. 5. The peaks are 0·594 (3) and 0·600 (3) e Å^{-3} for the Ag and Mo results respectively, with saddle points at the bond midpoints of heights 0·575 (4) and 0·577 (3) e Å^{-3} in each case. The peaks behind the nuclei in Fig. 5 have values of 0·391 (5) and 0·394 (5) e Å^{-3} for the Ag and Mo results respectively.

Comparison with other experimental results

There are few maps of $\Delta\rho(\mathbf{r})$ or $\rho_{val}(\mathbf{r})$ derived from experimental data with accuracy comparable with that of the present analysis. YC presented Fourier-summation maps of $\Delta\rho$ and ρ_{val} based on a data set consisting of the room-temperature Mo measurements of AH, four additional measurements by HKKK, and the 442 measurement of Trucano & Batterman (1972). The 222 value used by YC is *not* an experimental observation, but was derived by AH from an analysis of their data. Its magnitude, 1·352, is significantly smaller than the value used in the present analysis. No attempt was made by YC to correct for anharmonicity. The dispersion correction of $f' = 0{\cdot}1003$ employed for Mo radiation (Wagenfeld, Kuhn & Guttman, 1973) was larger than that used in the present analysis.

The Fourier deformation density map of YC (their Fig. 3) has features similar to those reported here, but the bond peak is ~0·29 e Å^{-3}. YC claim e.s.d.'s in their Fourier maps of 0·007 e Å^{-3}, which is unlikely

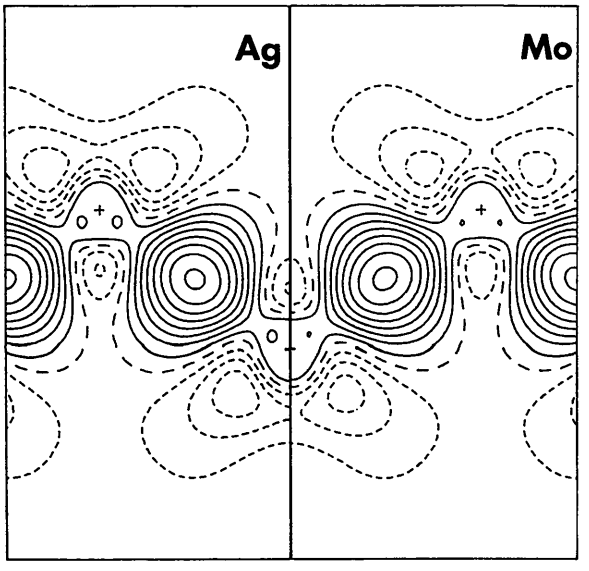

Fig. 4. Static deformation densities calculated from the pseudoatom models derived from both the Ag and Mo data. Nuclear positons are marked with a+. Contours as in Fig. 2. Map dimensions as in Fig. 1.

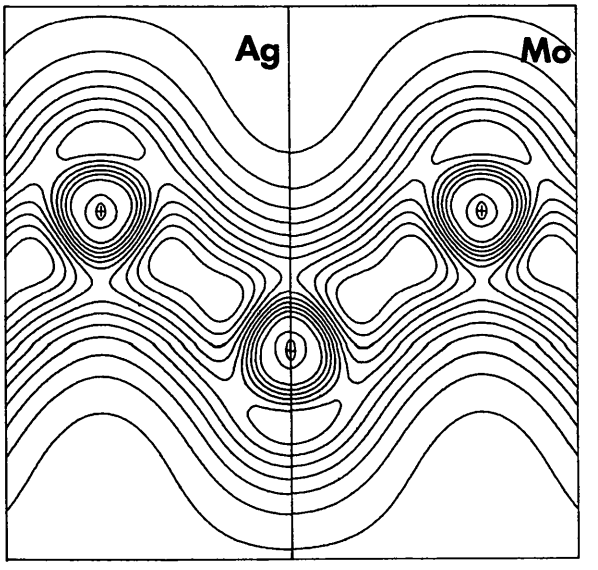

Fig. 5. Static valence densities calculated from the pseudoatom models derived from both the Ag and Mo data. Nuclear positions are marked with a+. Contours as in Fig. 3. Map dimensions as in Fig. 1.

given the inclusion of the four HKKK reflections of inferior accuracy. From the e.s.d.'s in the data used by YC (their Table 1) we obtain values of $\sigma(\Delta\rho)$ typically between 0·023 and 0·039 e Å^{-3}, in far better agreement with the 1·4% e.s.d.'s in the HKKK reflections. A similar estimate of $\sigma(\Delta\rho)$ (0·036 e Å^{-3}) was obtained by Scheringer (1980) for the YC results. The Fourier map of $\rho_{\rm val}(\mathbf{r})$ (Fig. 2 of YC) has a larger peak (0·69 e Å^{-3}) than those in Fig. 3 of the present work. Scheringer (1980) commented on these peak heights, concluding that they resulted from inaccuracy in the four HKKK reflections, an explanation we endorse.

A more subtle difference between the YC maps of $\rho_{\rm val}(\mathbf{r})$ and those in Fig. 3 is the shape of the bond peak. An elliptical shape is reported by YC, but it is clear from Fig. 3 that the peak is rectangular in shape. The elliptical peaks in Fig. 2 of YC appear to be due to the less-accurate HKKK reflections. Although we have used a density-localized *M*-shell function to obtain Fig. 3, this differs from the canonical function used by YC only in the core region, and hence is not the source of the discrepancy.

A model deformation density map has been reported by PMM (their Fig. 1) from pseudoatom refinement of the AH room-temperature Mo data. Their map was constructed from a Fourier summation of F_H^c *without* the 222 reflection. PMM obtain a peak height of only 0·13 e Å^{-3}. As noted by Scheringer (1980), the 222 reflection contributes ~0·07 e Å^{-3} to the bond peak. The inclusion of this reflection would yield a deformation density with a peak height similar to Fig. 2 of the present work.

Scheringer (1980) gives a Fourier-summed $\Delta\rho(\mathbf{r})$ map from a data set consisting of the 15 AH reflections employed by YC, with the 222 measurement of Roberto & Batterman (1970) and the 442 measurement of Trucano & Batterman (1972). The observations were phased by a bond-charge model, but were not corrected for anharmonicity. The bond peak of 0·20 e Å^{-3} obtained by Scheringer is comparable with those in Fig. 2 above, and Fig. 1 of that work is generally similar to our Fig. 2.

We have found no static model maps of $\Delta\rho$ or $\rho_{\rm val}$ derived from experimental data for silicon, except for the map of $\rho_{\rm val}$ by Stewart & Spackman (1981). The map in Fig. 6 of that work was obtained by methods similar to those used here. However, the model used was less flexible, and substantially underestimates the peak height in the bond (~0·47 e Å^{-3}).

Comparison with theory

Since we have obtained a representation of $\rho(\mathbf{r})$ commensurate with the accuracy of the experimental observations, it is appropriate to compare these results with theoretical calculations. We do this (i) by a comparison of theoretical $\Delta\rho(\mathbf{r})$ and (ii) $\rho_{\rm val}(\mathbf{r})$ maps with the model results above, and (iii) by a comparison of theoretical structure factors with a set of structure factors derived from the experimental measurements corrected for anharmonicity, dispersion effects and harmonic thermal motion.

(i) *Deformation density*

Only one theoretical calculation of $\Delta\rho(\mathbf{r})$ in bulk Si is known to us, that by Wang & Klein (1981). The bond peak obtained in that work is only ~0·16 e Å^{-3}, with a deficit behind the nucleus of ~−0·08 e Å^{-3}. The bond peak compares poorly with both the model and Fourier results obtained above.

Deformation density maps for Si_2 have been reported by Mrozek, Smith, Salahub, Ros & Rozendaal (1980) from calculations made with the $X\alpha-$SW, DV$-X\alpha$ and linear muffin-tin orbital methods. The agreement of the DV$-X\alpha$ deformation density with our model maps in Fig. 4 is remarkable. The bond peak is elliptical and extended perpendicular to the bond axis, with a maximum of 0·25 e Å^{-3}. The Si–Si distance in Si_2 (2·246 Å) is considerably shorter than that in bulk silicon (2·352 Å), which partly explains the higher peak obtained in the DV$-X\alpha$ calculation on Si_2.

(ii) *Valence density*

There are many theoretical maps of $\rho_{\rm val}(\mathbf{r})$ for silicon in the literature. Calculations of the electron density in solids typically assume a form of the core potential, and solve for the valence-electron density consistent with this potential. It is impossible to be exhaustive in our comparison with the model results in Fig. 5, but we discuss a number of results.

Chelikowsky & Cohen (1974) calculate the valence density in silicon using both local and nonlocal pseudopotentials. Both calculations yield valence densities with elliptical bond peaks, extended perpendicular (local pseudopotential) and parallel (nonlocal) to the bond. Both valence densities have single peaks of ~0·65 e Å^{-3} in the bond. These results are in poor agreement with our model results, in respect to both peak shape and peak heights. Similar maps of $\rho_{\rm val}(\mathbf{r})$ have been reported by Ihm & Cohen (1980), Baldereschi, Maschke, Milchev, Pickenhain & Unger (1981), Bertoni, Bortolani, Calandra & Nizzoli (1973) and Walter & Cohen (1971).

Hamann (1979) demonstrated that the single peak in the valence densities obtained by these authors largely results from their use of soft-core pseudopotentials. $\rho_{\rm val}(\mathbf{r})$ maps obtained by Hamann *via* use of both a hard-core pseudopotential (strongly repulsive near the nucleus) and a full potential both display rectangular bond contours, with a relatively flat maximum. However the maximum in $\rho_{\rm val}(\mathbf{r})$ between the nuclei was only 0·55 e Å^{-3}, somewhat less than the results in Fig. 5. Similar results have

been reported by Bachelet, Greenside, Baraff & Schluter (1981).

Zunger & Cohen (1979) and Zunger (1980) mapped ρ_{val} from a nonlocal pseudopotential using essentially hard-core pseudopotentials. Their map of $\rho_{val}(\mathbf{r})$ can be compared quantitatively with those in Fig. 5. Rectangular contours in the bond are elongated along the bond, with a long flat maximum of $\sim 0{\cdot}60$ e Å^{-3}. The peak behind the nuclei is 0·38 e Å^{-3}. These values compare favourably with the mean values from the maps in Fig. 5 of 0·576 and 0·393 e Å^{-3} at the bond midpoint and behind the nuclei respectively. However, the subtle twin-peaked nature of $\rho_{val}(\mathbf{r})$ in Fig. 5 is not reproduced.

Kenton & Ribarsky (1981) performed *ab initio* Hartree–Fock calculations on tetrahedrally coordinated Si_5H_{12} clusters in an attempt to mimic bulk silicon. Valence-density maps obtained for the Si–Si bond show a pronounced double peak, with a peak height of $\sim 0{\cdot}50$ e Å^{-3}, and heights at the bond midpoint of $\sim 0{\cdot}48$ e Å^{-3}. Although smaller in magnitude than the maps in Fig. 5, the double-peak nature of the *ab initio* results is supported by the present analysis.

The map of ρ_{val} reported by Wang & Klein (1981) compares favourably with the results in Fig. 5, having rectangular bond contours, with a plateau level of $\sim 0{\cdot}58$ e Å^{-3}, and a peak behind the nuclei of $\sim 0{\cdot}38$ e Å^{-3}. Allowing for the fact that we expect the core regions to differ, we find that the map reported by Wang & Klein (1981) is in excellent agreement with Fig. 5.

Finally, Yin & Cohen (1982, 1983) have published two similar maps, both from *ab initio* pseudopotential calculations. The earlier result (Yin & Cohen, 1982) shows rectangular bond contours, with a single bond peak of 0·59 e Å^{-3}, and a peak behind the nuclei of $\sim 0{\cdot}37$ e Å^{-3}. The more recent result shows a distinct, although subtle, twin peak in the bond, almost identical to those in Fig. 5. The peak values are 0·575 e Å^{-3}, with a saddle-point height of 0·565 e Å^{-3}. The peak behind the nuclei is 0·380 e Å^{-3}. Taken together, these results probably represent the closest agreement with the present model. It appears likely that subtle modifications of the computational procedure of Yin & Cohen (1980, 1982) would produce virtually exact agreement with Fig. 5.

(iii) *Comparison with theoretical structure factors*

Not all calculations of the electronic structure of bulk silicon report maps of either $\Delta\rho(\mathbf{r})$ or $\rho_{val}(\mathbf{r})$. However, most (including those which report such maps) report low-angle structure factors for comparison with experimental results. The experimental structure factors are usually corrected for thermal motion and anomalous dispersion effects. In some instances where this is claimed however, it is not in fact the case [*e.g.* experimental values reported by Zunger (1980) from AH have not been corrected for thermal motion].

Table 3. *Mean experimental structure factors for* Si, *corrected for anharmonicity, anomalous dispersion and harmonic thermal motion*

Values are normalized to a single Si atom. Figures in parentheses are e.s.d.'s in the last figures of $|F_{exp}|$.

h k l	$\lvert F_{exp}\rvert$	h k l	$\lvert F_{exp}\rvert$
1 1 1	10·737 (5)	4 4 0	6·051 (6)
2 2 0	8·659 (6)	4 4 4	4·983 (6)
3 1 1	8·024 (6)	5 5 1	4·812 (7)
2 2 2	0·193 (1)	6 4 2	4·558 (10)
4 0 0	7·449 (5)	8 0 0	4·178 (7)
3 3 1	7·251 (6)	6 6 0	3·873 (6)
4 2 2	6·719 (6)	5 5 5	3·776 (8)
3 3 3	6·425 (6)	8 4 4	3·148 (8)
5 1 1	6·445 (6)	8 8 0	2·546 (10)

To aid such comparisons, we determine a set of experimental structure factors from the mean Mo and Ag radiation data sets. To do this we correct the mean structure factors in each set for anomalous dispersion, using the experimental f' values of Deutsch & Hart (1984). These measurements of f' have associated e.s.d.'s of 4·7 and 2·1% for the Ag and Mo corrections respectively, and the values of $\sigma(|F|)$ are increased accordingly. Using these increased e.s.d.'s, we construct a weighted mean of the two data sets. The mean B value obtained from the two pseudoatom refinements is used to correct the structure factors for thermal motion, and the e.s.d. in the temperature-factor correction is included in the final e.s.d.'s. The resulting structure factors, normalized to one silicon atom, and their associated e.s.d.'s, are given in Table 3. The value for the 222 reflection is derived solely from the measurement of Alkire *et al.* (1982). We have omitted the 442 and 622 reflections; these are discussed separately below.

Using the experimental values in Table 3, we can compare the various theoretical calculations with experiment. We compare twelve calculations of structure factors, either for the total electron density, or for the valence density. These are taken from Yin & Cohen (1982), Dovesi, Causa & Angonoa (1981), Wang & Klein (1981), Heaton & Lafon (1981), Zunger (1980), Zunger & Cohen (1979), Tejedor & Verges (1979), Chelikowsky & Cohen (1974) and Stukel & Euwema (1970). These publications report varying numbers of structure factors, and in the cases of Tejedor & Verges (1979) and Chelikowsky & Cohen (1974) only valence density structure factors. To these we add core contributions obtained from the density-localized K and L shells used for the pseudoatom refinements (Stewart, 1980). We include both the local and nonlocal pseudopotential results from Chelikowsky & Cohen (1974), and four sets of results

Table 4. *Unweighted R factors for agreement between twelve theoretical structure-factor determinations, and the mean experimental values in Table 3*

N is the number of reflections compared in each case.

Calculation reference	$100 \times R$	N
Yin & Cohen (1982)	1·12	10
Dovesi *et al.* (1981)	0·73	11
Wang & Klein (1981)	0·50	10
Heaton & Lafon (1981)	0·45	8
Zunger & Cohen (1979); Zunger (1980)	1·49	10
Tejedor & Verges (1979)	0·94	10
Chelikowsky & Cohen (1974) local	1·19	10
Chelikowsky & Cohen (1974) nonlocal	0·77	10
Stukel & Euwema (1970) Sl	1·45	11
Stukel & Euwema (1970) KSG	0·43	11
Stukel & Euwema (1970) Sl-RHF	0·35	11
Stukel & Euwema (1970) KSG-RHF	0·35	11

from Stukel & Euwema (1970), labelled by those authors as Sl, KSG, Sl-RHF and KSG-RHF.

In Table 4 we compare unweighted R factors ($R = \sum ||F_{exp}| - |F_{theor}|| / \sum |F_{exp}|$) for these theoretical calculations. Although most calculations are claimed to be in good agreement with experiment, the R factor is surprisingly poor in some cases. In particular, agreement factors obtained for the data sets of Yin & Cohen (1982) and Zunger & Cohen (1979; Zunger, 1980) of 1·12 and 1·49% respectively are not in accord with the excellent agreement reported above between their maps of $\rho_{val}(\mathbf{r})$ and the experimental results. Closer inspection reveals that, for these two sets of structure factors, $|F_{exp}|$ always exceeds $|F_{theor}|$. The difference is as large as 0·22 electrons for the 331 reflection, and persists for the highest-angle reflection reported (440). Such a systematic discrepancy strongly suggests an inappropriate core contribution added to the Fourier-transformed valence densities obtained by these authors. A systematic difference is also seen in the Sl set of Stukel & Euwema (1970), where $|F_{exp}|$ is uniformly less than $|F_{theor}|$. Such errors prevent us from making strong conclusions based on agreement indices alone.

Based on the R factors in Table 4, three sets by Stukel & Euwema (1970) and those by Heaton & Lafon (1981) and by Wang & Klein (1981) stand out from the rest. The Hartree–Fock calculation of Dovesi *et al.* (1981) is noticeably inferior, as it substantially overestimates all key low-angle reflections, while underestimating the important 222 reflection by 40%.

The 442 and 622 reflections

The measurements of the weak 442 and 622 reflections used in our pseudoatom refinements and Fourier analyses are from Tischler & Batterman (1984), corrected for anharmonicity by those authors. It is evident from the residuals listed in Table 2 that our model is a very poor fit to these data points, $\Delta|F|$ being typically $10\sigma(|F|)$ for both reflections. This is worrying since the measurements of Tischler & Batterman (1984) agree with earlier results of Mills & Batterman (1980) and Trucano & Batterman (1972).

As noted by Tischler & Batterman, the structure factors of these reflections (for which $h+k+l = 4n+2$) result from both the antisymmetric electron distribution vibrating harmonically and the centrosymmetric electron distribution vibrating anharmonically. The sum of these two contributions is measured experimentally, and is evidently reproducible. However, the correction of these values for anharmonic effects is not as straightforward as indicated by Tischler & Batterman (1984). These authors appear to use values of the anharmonic force constant, β, from the measurements of Hastings & Batterman (1975). These values, 1·61 and 1·38 eV Å^{-3}, are derived from the high-temperature (*i.e.* above room temperature) behaviour of the neutron 442 and 622 reflections respectively. They are substantially less than the value of 3·38 eV Å^{-3} obtained from the room-temperature neutron 222 reflection, and used for anharmonicity corrections in this work. It is possible that β at room temperature may differ from β at higher temperatures due to a breakdown of the one-particle-potential approximation (Mair, private communication).

To ascertain the effect on the anharmonicity-corrected structure factors, we rescale the corrections applied by Tischler & Batterman by the ratio of β values appropriate to each reflection. This yields $F_{442}^{bond} = -0{\cdot}0926$ and $F_{622}^{bond} = -0{\cdot}0240$, compared with the values of $-0{\cdot}0635$ and $-0{\cdot}0046$ reported by these authors. These substantially different estimates are in excellent agreement with the mean of the values obtained from the model refinements ($-0{\cdot}093$ and $-0{\cdot}025$ for the 442 and 622 reflections respectively). Not only are the magnitudes predicted well by the model, but the signs of both reflections are in agreement with experiment. These modified values of F^{bond} are also in better accord with the theoretical values reported by Tischler & Batterman from the *ab initio* pseudopotential calculation of Yin & Cohen (1982) ($-0{\cdot}084$ and $-0{\cdot}020$ for the 442 and 622 reflections respectively), although it is not clear whether the theoretical values include the Debye–Waller factor; the original work of Yin & Cohen (1982) does not report structure factors for the 442 and 622 reflections.

If similar considerations are applied to the measurements of the Ge 442 and 622 reflections by Tischler & Batterman, it is quite likely that the sign of the Ge 442 structure factor would become negative, in agreement with the result of Yin & Cohen (1982). Far from yielding an unambiguous change of sign in F_{442}^{bond} between Si and Ge as claimed by Tischler & Batterman, the uncertainty over which value of β to use for the anharmonicity correction precludes a definitive conclusion.

The model results for the 442 and 622 structure factors indicate that the pseudoatom refinement used in the present analysis of the experimental data yields a reliable representation of the static electron distribution in bulk silicon. The weak $4n+2$ reflections are reproduced accurately, both in phase and magnitude, if we accept the more appropriate room-temperature anharmonicity correction for the 442 and 622 reflections. This is not the case for the simple bond-charge model employed by Scheringer (1980), which yields values of +1·419 and +0·025 for the 222 and 442 reflections respectively. This underestimates the 222 structure factor, and predicts the wrong sign for the 442 reflection. The use of bond-charge models for the analysis of accurate diffraction data therefore appears to be limited to the description of the gross features for which it was devised (*i.e.* bond charges). It is inadequate for the description of the more subtle features of the electron density distribution.

Summary

The major conclusions of the analysis of the experimental data are:

(i) $\Delta\rho(\mathbf{r})$ for silicon is characterized by an elliptical bond peak, elongated perpendicular to the bond. The peak height (from the pseudoatom model) is 0·206 (3) e Å^{-3}. There is a corresponding region of deficit of electron density behind the nuclei, peaking along [111], with maximum depth −0·090 (4) e Å^{-3}.

(ii) The valence density derived from the pseudoatom model displays a distinct twin peak in the bond. The peaks are located 0·85 Å from the nucleus, with a height of 0·597 (3) e Å^{-3}; the saddle point at the bond midpoint has a value of 0·577 (3) e Å^{-3}. The peak behind the nuclei reaches 0·393 (5) e Å^{-3}.

(iii) The valence density derived from a Fourier summation shows a single peak in the bond, with height 0·613 (6) e Å^{-3}. This is an artefact of the effects of both thermal motion and series termination.

(iv) The two mean data sets, Ag and Mo, give essentially identical results, both from Fourier summations and model fitting.

(v) There are systematic residuals after model fits to both data sets, of approximately the same magnitude as the experimental e.s.d.'s in the observations. Similar residuals are observed in model refinements of the low-temperature data of AH (both Ag and Mo sets), and suggest *L*-shell deformations, both spherical and aspherical, which were not included in the model.

(vi) The weak 442 and 622 reflections measured by Tischler & Batterman (1984) appear to have been corrected for anharmonicity with an inappropriate value of β, the cubic anharmonic force constant.

A detailed comparison of the derived experimental electron distributions has been made with a large number of theoretical determinations of the electron distribution. Salient features of this comparison are:

(i) There appear to be errors in the computation of structure factors from theoretical electron densities in the work of Yin & Cohen (1982), Zunger (1980), Zunger & Cohen (1979) and Stukel & Euwema (1970; Sl set only). These can be attributed to the use of an inappropriate core scattering factor. It is suggested that the density-localized core functions of Stewart (1980) are appropriate for this purpose, as they are compatible with the nodeless valence-electron densities in the theoretical calculations.

(ii) The best agreement with experiment is obtained with the *ab initio* pseudopotential method of Yin & Cohen (1980, 1982, 1983), notwithstanding the computational errors described above. Excellent agreement with experiment is also obtained for the calculations of Zunger (1980), Zunger & Cohen (1979), Heaton & Lafon (1981), Wang & Klein (1981) and Stukel & Euwema (1970; KSG, Sl-RHF and KSG-RHF sets). The calculation by Dovesi *et al.* (1981) predicts the correct topography of $\Delta\rho$ and $\rho_{\rm val}$, but consistently underestimates the magnitude of the features.

(iii) The single-peak valence densities reported by Chelikowsky & Cohen (1974) are the result of the use of soft core pseudopotentials (Hamann, 1979), and are not supported by the present experimental analysis.

We believe that the results we have derived from experimental data, and presented in Figs. 2 through 5, currently provide the best possible representation of the electron distribution is silicon. They are superior to the results of Yang & Coppens (1974).

The author is grateful to Dr E. N. Maslen for invaluable discussions, and to Drs S. L. Mair and H. P. Weber and Mr R. G. Nanni for a critical reading of the manuscript. This work was supported by the Australian Research Grants Scheme.

Note added in proof: Subsequent to submission of the manuscript, Deutsch & Hart (1985*a*, *b*) published accurate structure factors for eight reflections. No attempt has been made to incorporate these measurements into the above analysis. Three of the reflections are common to the present data set, but the remaining five yield virtually no information on the valence-electron distribution, since they lie in the range $1{\cdot}04 < \sin\theta/\lambda < 1{\cdot}56$ Å^{-1}. They do however provide further insight into thermal motion and *K*- or *L*-shell polarization in silicon. Deutsch & Hart (1985*b*) derive $B =$ 0·4632 (41) Å^2 from the three lowest-angle measurements, in exact agreement with the mean value of 0·4632 (11) Å^2 obtained in the analysis above. A larger B value of 0·5085 (35) Å^2 is obtained from the three highest-angle reflections, suggesting a different thermal motion for the *K* and *L* shells. Those authors

also find no anharmonic contribution to the structure factors within the accuracy of the experiment, in contradiction of the analysis above. The neglect of an anharmonicity correction in the present work would make a trivial difference to the resulting electron distribution; it is not of critical importance.

References

ALDRED, P. J. E. & HART, M. (1973). *Proc. R. Soc. London, Ser. A*, **332**, 223-238, 239-254.

ALKIRE, R. W., YELON, W. B. & SCHNEIDER, J. R. (1982). *Phys. Rev. B*, **26**, 3097-3104.

BACHELET, G. B., GREENSIDE, H. S., BARAFF, G. A. & SCHLUTER, M. (1981). *Phys. Rev. B*, **24**, 4745-4752.

BALDERESCHI, A., MASCHKE, K., MILCHEV, A., PICKENHAIN, R. & UNGER, K. (1981). *Phys. Status Solidi B*, **108**, 511-520.

BECKER, P., SEYFRIED, P. & SIEGERT, H. (1982). *Z. Phys. B*, **48**, 17-21.

BERTONI, C. M., BORTOLANI, V., CALANDRA, C. & NIZZOLI, F. (1973). *J. Phys. C*, **6**, 3612-3630.

CHELIKOWSKY, J. R. & COHEN, M. L. (1974). *Phys. Rev. B*, **10**, 5095-5107.

CLEMENTI, E. (1965). *IBM J. Res. Dev.* **9**, Suppl. 2.

COPPENS, P., GURU ROW, T. N., LEUNG, P., STEVENS, E. D., BECKER, P. J. & YANG, Y. W. (1979). *Acta Cryst.* A**35**, 63-72.

CREAGH, D. (1984). *Phys. Lett. A*, **103**, 52-56.

CROMER, D. T. & LIBERMAN, D. J. (1970). *J. Chem. Phys.* **53**, 1891-1898.

CUSATIS, C. & HART, M. (1975). In *Anomalous Scattering*, edited by S. RAMASESHAN & S. C. ABRAHAMS, pp. 57-68. Munksgaard: Copenhagen.

DAWSON, B. (1967). *Proc. R. Soc. London Ser. A*, **298**, 264-288, 379-394.

DAWSON, B., HURLEY, A. C. & MASLEN, V. W. (1967). *Proc. R. Soc. London Ser. A*, **298**, 289-306.

DEUTSCH, M. & HART, M. (1984). *Phys. Rev. B*, **30**, 640-642.

DEUTSCH, M. & HART, M. (1985*a*). *Acta Cryst.* A**41**, 48-55.

DEUTSCH, M. & HART, M. (1985*b*). *Phys. Rev. B*, **31**, 3846-3858.

DOVESI, R., CAUSA, M. & ANGONOA, G. (1981). *Phys. Rev. B*, **24**, 4177-4183.

FEHLMANN, M. (1979). *J. Phys. Soc. Jpn*, **47**, 225-231.

HAMANN, D. R. (1979). *Phys. Rev. Lett.* **42**, 662-665.

HANSEN, N. K. & COPPENS, P. (1978). *Acta Cryst.* A**34**, 909-921.

HASTINGS, J. B. & BATTERMAN, B. W. (1975). *Phys. Rev. B*, **12**, 5580-5584.

HATTORI, H., KURIYAMA, H., KATAGAWA, T. & KATO, N. (1965). *J. Phys. Soc. Jpn*, **20**, 988-996.

HEATON, R. & LAFON, E. (1981). *J. Phys. C*, **14**, 347-351.

IHM, J. & COHEN, M. L. (1980). *Phys. Rev. B*, **21**, 1527-1536.

KEATING, D., NUNES, A., BATTERMAN, B. & HASTINGS, J. (1971). *Phys. Rev. B*, **4**, 2472-2478.

KENTON, A. C. & RIBARSKY, M. W. (1981). *Phys. Rev. B*, **23**, 2897-2910.

MILLS, D. & BATTERMAN, B. W. (1980). *Phys. Rev. B*, **22**, 2887-2897.

MROZEK, J., SMITH, V. H., SALAHUB, D. R., ROS, P. & ROZENDAAL, A. (1980). *Mol. Phys.* **41**, 509-517.

PRICE, P. F., MASLEN, E. N. & MAIR, S. L. (1978). *Acta Cryst.* A**34**, 183-193.

ROBERTO, J. B. & BATTERMAN, B. W. (1970). *Phys. Rev. B*, **2**, 3220-3226.

ROBERTO, J. B., BATTERMAN, B. W. & KEATING, D. T. (1974). *Phys. Rev. B*, **9**, 2590-2599.

SCHERINGER, C. (1980). *Acta Cryst.* A**36**, 205-210.

SPACKMAN, M. A., HILL, R. J. & GIBBS, G. V. (1986). *Phys. Chem. Miner.* Submitted.

SPACKMAN, M. A. & MASLEN, E. N. (1985). *Acta Cryst.* A**41**, 347-353.

SPACKMAN, M. A. & STEWART, R. F. (1984). In *Methods and Applications in Crystallographic Computing*, edited by S. R. HALL & T. ASHIDA, pp. 302-320. Oxford Univ. Press.

SPACKMAN, M. A. & STEWART, R. F. (1986). In preparation.

STEWART, R. F. (1973). *J. Chem. Phys.* **58**, 1668-1676.

STEWART, R. F. (1976). *Acta Cryst.* A**32**, 565-574.

STEWART, R. F. (1980). In *Electron and Magnetization Densities in Molecules and Crystals*, edited by P. BECKER, pp. 427-431. New York: Plenum Press.

STEWART, R. F. & SPACKMAN, M. A. (1981). In *Structure and Bonding in Crystals*, Vol. 1, edited by M. O'KEEFFE & A. NAVROTSKY, pp. 279-298. New York: Academic Press.

STUKEL, D. J. & EUWEMA, R. N. (1970). *Phys. Rev. B*, **1**, 1635-1643.

TEJEDOR, C. & VERGES, J. A. (1979). *Phys. Rev. B*, **19**, 2283-2290.

TEWORTE, R. & BONSE, U. (1984). *Phys. Rev. B*, **29**, 2102-2108.

TISCHLER, J. Z. & BATTERMAN, B. W. (1984). *Phys. Rev. B*, **30**, 7060-7066.

TRUCANO, P. & BATTERMAN, B. W. (1972). *Phys. Rev. B*, **6**, 3659-3666.

WAGENFELD, H., KUHN, J. & GUTTMAN, A. J. (1973). Proc. First Eur. Crystallogr. Meet., Bordeaux.

WAL, R. J. VAN DER & STEWART, R. F. (1984). *Acta Cryst.* A**40**, 587-593.

WALTER, G. P. & COHEN, M. L. (1971). *Phys. Rev. B*, **4**, 1877-1892.

WANG, C. S. & KLEIN, B. M. (1981). *Phys. Rev. B*, **24**, 3393-3416.

WILLIS, B. T. M. & PRYOR, A. W. (1975). *Thermal Vibrations in Crystallography*. Cambridge Univ. Press.

YANG, Y. W. & COPPENS, P. (1974). *Solid State. Commun.* **15**, 1555-1559.

YIN, M. T. & COHEN, M. L. (1980). *Phys. Rev. Lett.* **45**, 1004-1007.

YIN, M. T. & COHEN, M. L. (1982). *Phys. Rev. B*, **26**, 5668-5687.

YIN, M. T. & COHEN, M. L. (1983). *Phys. Rev. Lett.* **50**, 1172.

ZUNGER, A. (1980). *Phys. Rev. B*, **21**, 4785-4790.

ZUNGER, A. & COHEN, M. L. (1979). *Phys. Rev. B*, **20**, 4082-4108.